

Processing and characterization of pure cordierite and zirconia-doped cordierite ceramic composite by precipitation technique

M SENTHIL KUMAR^{1,*}, A ELAYA PERUMAL², T R VIJAYARAM¹ and GOVINDAN SENGUTTUVAN³

¹School of Mechanical and Building Sciences, VIT University, Chennai 600 127, India

²Department of Mechanical Engineering, Anna University, Chennai 600 025, India

³Department of Physics, College of Engineering and Technology, Tiruchirappalli 620 024, India

MS received 3 January 2014; revised 1 August 2014

Abstract. Pure cordierite and cordierite–ZrO₂ composite (5–20 wt%) ceramics for various stoichiometric compositions were synthesized from standard raw materials by a novel precipitation technique. The analytical techniques such as X-ray diffraction, simultaneous thermogravimetric and differential thermal analysis, Fourier transform infrared spectroscopy, scanning electron microscopy and bulk density were employed to evaluate the properties and microstructure. Results show that the ceramic composites consist of cordierite and zircon phases. The cordierite–zirconia (20 wt%) increased the fracture toughness value from 3.38 to 3.94 MPa, which is mainly due to martensitic transformation present in zirconia. The flexural strength of composite was found to increase from 126.46 to 297.62 MPa. The thermal expansion coefficients of cordierite and cordierite–zirconia (20 wt%) were 4.08×10^{-6} and $4.42 \times 10^{-6} \text{ }^{\circ}\text{C}^{-1}$ which may be due to the addition of zirconia.

Keywords. Cordierite; zirconia (ZrO₂); temperature; phase transformation; properties.

1. Introduction

The mechanical properties play a major role in determining the suitability of any material for specific applications in engineering applications. The desirable properties of ceramic systems are obtained by proper selection of the stoichiometric composition needed for the formation of crystalline phases. Fine-grain developed microstructure improves the thermo-mechanical properties,¹ in high temperature applications like kiln furniture, molten metal filter, microelectronic components and industrial heat recovery.² Cordierite ceramic is used increasingly in thermal-related applications due to its low thermal expansion and high refractoriness. Cordierite ceramic have lower cost of operation, chemically inert, high reliability and durability, low pressure drop, fast heating time and structural stability at high temperatures. This is a requirement for thermal shock resistance and for use in severely exhaustive environments at high temperatures.³ The impetus of cordierite research activity is mainly due to their prominence in the current market scenario.

There have been different synthesis procedures for cordierite ceramic like conventional and unconventional techniques (sol–gel, precipitation, co-precipitation, etc.). The conventional method described for synthesizing cordierite ceramic is carried out by using naturally available materials like kaolin and talc for specific application in casting⁴ and also by two different methods (mechanical and precipitation

technique) by using nonstandard raw materials kaolin, talc, feldspar, silica and sepiolite for foundry application.⁵ Researchers have also prepared pure cordierite powders through the sol–gel technique.⁶ The mechanochemical activation performed on starting materials kaolin, pyrophyllite and talcum showed synthesis by solid-state reaction occurred at lower sintering temperature, also reported low thermal expansion.⁷

Cordierite is not easily obtained by solid-state reactions from oxides, because of its refractory character. Synthetic powders exhibit heterogeneous surface properties and even chemical inhomogeneity. Hence for better homogeneous mixture, the addition of sintering aids or impurities was introduced. The final (especially mechanical) characteristics of a ceramic body are strongly dependent on the nature of the starting powder, an improvement in the reliability and reproducibility of cordierite properties is highly desirable. The powders synthesized without sintering aid reported either very low or no improvement in mechanical properties thus proved that it is difficult to promote sintering without a sintering aid. This was due to its narrow sintering range around 1420°C and has its incongruent melting at 1450°C.⁸ The use of sintering aid results in lowering of the crystallization temperature and increases the thermal expansion coefficient thus making it difficult to produce a high density and high strength cordierite ceramic material.

Cordierite has relatively poor mechanical properties compared to other ceramic materials, and in order to enhance its mechanical properties, zirconia, titania, ceria, etc., have been added to the cordierite matrix as a secondary phase. The interaction between cordierite and copper and/or cerium

*Author for correspondence (msv305@yahoo.co.in, ep_mal@yahoo.com)

oxides revealed that copper oxide had reacted at 900°C with the formation of a new phase (the spinel, CuAl_2O_4); on the contrary cerium oxide does not react up to 1200°C.⁹ Modifications in the microstructure and mechanical properties of ceria-doped cordierite have been investigated from minerals such as kaolin, talc and alumina, slurried with water and plasticizers.¹⁰ Cordierite–titania synthesized from talc and clay produced materials with reduced thermal expansion.¹¹ Gel cast forming method using tert-butyl alcohol improved the low temperature sintering of the cordierite powder.¹² Cordierite formation was observed at low sintering temperature (1300°C) with the addition of TiO_2 dopant. Titania-doped cordierite exhibited better mechanical properties and low thermal expansion coefficient. The addition of the dopant showed a remarkable influence on crystallization.¹³

There are wide ranges of techniques available, and each requires different characteristics in the starting powder. Therefore it is essential that the production processes are capable of being controlled to produce the desired properties, and characterization techniques exist to be able to monitor them. For these reasons, an alternative method for processing by chemical route, ‘precipitation process’ that would yield highly reactive and better controlled cordierite particles, have been developed.

The precipitation technique using aluminium sulphate, magnesium sulphate and sodium silicate solution with zirconia powder between 15 and 35 wt% resulted in highly densified cordierite. The results showed good sintering characteristics with improved mechanical properties at zirconia composition of 15 wt%.¹⁴ The reports suggested that the cordierite matrix dispersed with fine zirconia (ZrO_2) increased the mechanical properties but affect the sinterability of the composites¹⁵ and the dispersion of ZrO_2 particles as a second phase enhanced the mechanical properties of cordierite.¹⁶

The present research work is focused on the synthesis of highly homogeneous cordierite and cordierite–zirconia (5–20 wt%) ceramic. The ceramic composites were prepared from standard raw materials by the precipitation technique, novel technique for synthesis. The physical, thermo-mechanical properties were investigated to evaluate the porosity, density, hardness, fracture toughness, flexural strength and coefficient of thermal expansion. The proposed research is carried out to examine its possibility as an alternate material for high temperature applications.

2. Materials and methods

2.1 Sample preparation

Synthesizing by precipitation technique of cordierite and cordierite–zirconia was done with a stoichiometric composition of cordierite (MgO : 13.8 wt%, Al_2O_3 : 34.8 wt%, SiO_2 : 51.4 wt%) and zirconia (5–20 wt%). Oxides of the starting powders were mixed with water as the solvent and sodium hydroxide, and then precipitated with sodium carbonate and hydrochloric acid. The precipitate was filtered and washed

until the presence of Na^+ is diminished. The precipitate was dried at 100°C for 12 h. The cordierite–zirconia samples were added with zirconia (5–20 wt%). The samples were wet milled for 3 h and dried at 100°C for 12 h. Then it was followed by dry milling at 2 h. The dried sample powders were added with 1 wt% flux. The precursor powders were then uniaxially pressed into pellets and round bars at 240 MPa to 10 mm in diameter, using 1 wt% of polyvinyl alcohol (PVA) as a binder. The green compacts were calcined at 400°C for 3 h at a slow heating rate 2°C min^{-1} to avoid uneven shrinkage, bending and to burnout the binder. The calcined compacts were sintered at different temperatures between 1000 and 1350°C for 3 h.

2.2 Characterization

The prepared samples were characterized by diffractometer (XRD 3000, SEIFERT) with a graphite monochromatic $\text{Cu-K}\alpha$ radiation of 1.5406 Å operating at 30 kV and 40 mA to study the X-ray powder diffraction (XRD). The XRD patterns were acquired in the 2θ range of 5–70° to determine the phase evolution at different sintering temperatures. The thermogravimetric and differential thermal analysis (TG/DTA) curve was obtained from the thermal analyzer (NETZSCH STA 409 C/CD TG/DTA Instrument) at a heating rate of $10^\circ\text{C min}^{-1}$, to study the thermal decomposition and phase evolution of the dried powders. The structural deformation and bonding nature of the heat-treated powders, obtained by the Fourier transform infrared (FTIR) spectrometer (BRUKER RFS27) in potassium bromide (KBr) medium were recorded in the range 4000–50 cm^{-1} are explained.

2.3 Sintering and microstructure

The samples were sintered for 3 h in air at different temperatures ranging from 1000 to 1350°C. The heating rate was chosen as $10^\circ\text{C min}^{-1}$ up to the sintering temperatures for all samples. Natural cooling (5°C min^{-1}) was maintained after the soaking period. The density of the sintered samples was determined by applying the Archimedes principle and porosity analysis was carried out by using computer integrated image analyser. The sintered samples were then polished by using different grades of polishing sheets (1/0–4/0). The mirror polished specimens were thermally etched at 1200°C for 30 min. Finally, the polished powders were subjected to study the morphological features by means of the scanning electron microscope (SEM HITACHI-S3400N) micrographs.

2.4 Thermo-mechanical properties

Hardness measurement was carried out on thermally etched samples by the Vickers indentation technique (Model ZWICK 3212) for a standard load of 98 N¹³ in the microhardness tester. The fracture toughness (K_{IC}) was evaluated by using the indentation fracture method. The K_{IC} of the ceramics was estimated for a load (98 N), for 15 s as the holding time experimentally, using the following formula¹⁷ with a

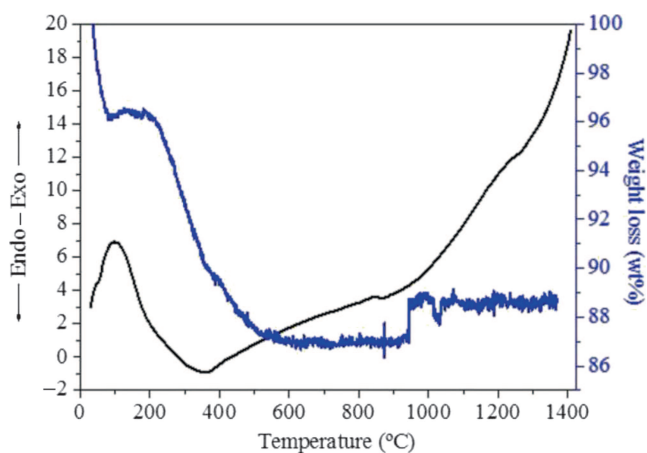


Figure 1. TG/DTA curve for pure cordierite sample dried at 100°C.

Vickers indenter:

$$K_{IC} = (0.0319 \times P) / a l^{1/2}$$

where P is the indentation force (N), c the crack length (m) and a the half-length of the diagonal (m), $l = c - a$, as described in figure 1.

The flexural strength was measured by using 5 samples in each composition prepared with a span length of a 25 mm long. The measurements were performed using the three-point bending technique, using a universal testing machine (Model Unitek-94100, Fuel instrument and Engineers). The cross head speed in loading was 0.5 mm min⁻¹. The thermo-mechanical analysis was carried out by using a dilatometer (Model Dil/1400C, VB Ceramics). The coefficient of thermal expansion was measured at a heating rate of 10°C min⁻¹ from 70 to 800°C.

3. Results and discussion

3.1 Characterization studies for cordierite and cordierite–zirconia ceramic samples

The characterization results for the samples of cordierite and cordierite–zirconia (5–20 wt%) ceramic composite, at different sintering temperatures are shown in table 1. The results exhibited the importance of sintering temperature in the synthesis of cordierite and cordierite–zirconia samples. Further, the results revealed the phase transformations at different temperatures. It also confirmed the presence of pure cordierite as a primary phase and zircon as a secondary phase in the cordierite–zirconia samples.

3.1a Thermal evaluation (TGA/DTA): The cordierite powder sample was subjected to TG/DTA analysis and the curve obtained is shown in figure 1. Two endothermic peaks were observed in two regions in the pure cordierite sample

Table 1. Phase evolution of samples at various sintering temperatures.

Sample	Phase composition				
	600°C	800°C	1000°C	1200°C	1350°C
Cordierite	A	MAS	μ-C S C	μ-C α-C S C	α-C
Cordierite–zirconia (5 wt%)	A	MAS	μ-C S C t-Zir	μ-C α-C S C t-Z	α-C Z
Cordierite–zirconia (10 wt%)	A	MAS	μ-C S C t-Zir	μ-C α-C S C t-Z	α-C Z
Cordierite–zirconia (15 wt%)	A	MAS	μ-C S C t-Zir	μ-C α-C S C t-Z	α-C Z
Cordierite–zirconia (20 wt%)	A	MAS	μ-C S C t-Zir	μ-C α-C S C t-Z	α-C Z

A—amorphous; MAS—magnesium aluminium silicate; μ-C—cordierite (metastable); S—spinel; C—cristobalite; Z—zircon; t-Zir—tetragonal zirconia; α-C—cordierite (stable).

(PCZr0). The first weight loss was observed in the temperature range between 150 and 250°C, it indicated the release of physically absorbed water and the second weight loss at 500°C was due to the dehydration of alumina.¹² The exothermic peak between 800 and 850°C indicated the initiation of solid-state reaction that leads to phase transformation. The second exothermic peak between 897 and 964°C and the third peak at 1332°C^{18,19} confirmed the formation of an intermediate phase (μ-cordierite) and final phase (α-cordierite), respectively.

TG/DTA analysis revealed that the cordierite–zirconia (PCZr5–PCZr20) samples were decomposed in the temperature range of 500–900°C. The TG/DTA curve for cordierite–zirconia (PCZr20) shown in figure 2 exhibited an exothermic peak between 750 and 800°C, which confirmed the presence of the solid-state reaction. The second exothermic peak around 950–1100°C may be due to the crystallization of the amorphous phase to intermediate phase (μ-cordierite)¹² and the final transformation phase (α-cordierite).¹⁸ The results

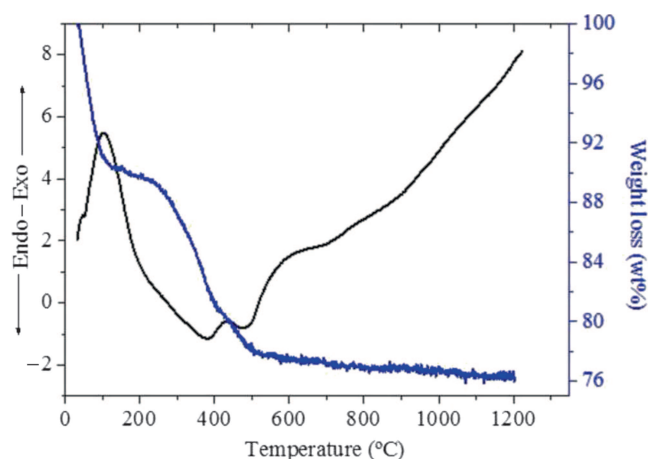


Figure 2. TG/DTA curve for cordierite-zirconia (PCZr20) sample dried at 100°C.

show the formation of cordierite at temperature lesser than the crystallization temperature.

The above results were in agreement with the results of previous research work,²⁰ that reported the crystalline phase of cordierite phase transformation. The precursor powders were heat treated up to 1200°C for different series of DTA curves. The crystallization began between 929 and 1100°C; the first peak at 929 to 934°C is due to the formation of the metastable phase of stuffed β -quartz, and the second peak is due to a trace amount of spinel. The third exothermic peak is due to the phase transformation of stuffed α -quartz to μ -cordierite.

3.1b FTIR characterization: Figure 3 shows the FTIR spectrum for pure cordierite powder (PCZr0). At 100°C, the absorption band of SiOH and/or AlOH group at 813 cm^{-1} diminished with the increase in temperature. It indicated that the condensation rate proceeds with heating. The absorption intensity of the AlO_4 band was found to be increasing with temperature. It is also observed that the Si-O-Al band at 1086 cm^{-1} also shifts to a lower wave number. From the experimental results, it is apparent that AlO_6 transformed into AlO_4 during precursor heating.²¹ The aluminium ions get incorporated into SiO_4 tetrahedral unit to form a Si-O-Al network structure.²¹

FTIR spectra of the cordierite powder at 1200°C show peaks at 1079, 956 and 486 cm^{-1} , which is typical for the adsorption bands of silica bonds and μ -cordierite.²² The band near 1100 cm^{-1} is due to stretched bond motion of Si atom against its tetrahedral oxygen cage, while the band near 486 cm^{-1} correspond to a symmetric motion of bridged oxygen in the plane bisecting the Si-O-Si bond.²³

The presence of non-bridged oxygen in the vibration mode in aluminosilicate at Mg content is observed in band at 945 cm^{-1} .²⁴ The absorption band at 740 cm^{-1} corresponds to the stretched vibration modes of Al-O and Mg-O bonds.²⁵ The spectra of the powder heat treated at 1200°C correspond to a mixture of solid solution and spinel phase. The existence

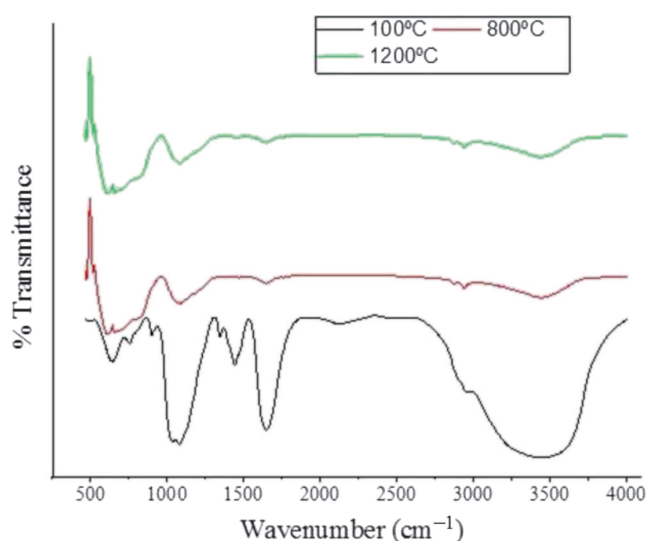


Figure 3. FTIR spectrum of pure cordierite sample at different sintering temperatures.

of spinel is evident due to the presence of bands at 650 and 550 cm^{-1} .²⁶ The absorption bands at 1080 and 776 cm^{-1} were due to the presence of hexagonal β -quartz and μ -cordierite at higher sintering temperature.²⁷

Figure 4 shows FTIR spectrum of the cordierite-zirconia (PCZr20) sample at different sintering temperatures. The presence of Si-O-Si in asymmetric stretched mode due to vibrations observed in bands at 900, 1010 and 1100 cm^{-1} for the sample calcined at 100°C. Symmetric stretching of AlO_4 tetrahedra occurred at band 1300 cm^{-1} . It should be the band at around 740 cm^{-1} at 100°C was due to the symmetric stretching mode of the Si-O-Si bond in the sample. The band at 700 and 760 cm^{-1} shows the vibration mode of Al-O or Mg-O, also the band at 1090 cm^{-1} corresponds to AlO_4 tetrahedra. The band between 1090 and 1270 cm^{-1} confirms the presence of SiO_4 at 800°C. The presence of μ -cordierite and α -cordierite is confirmed at bands 1300, 1100, 870 and 580 cm^{-1} at 1200°C. The presence of ZrO_2 is confirmed at 530 cm^{-1} .²⁸ The results of FTIR samples were consistent with X-ray diffraction results. The studied adsorption bands reveal the results of the IR spectrum of cordierite samples at different temperatures. At lower temperatures, these bands were similar to the spectrum of cordierite glass. The sample heated at 1000 and 1100°C shows the vibration of M-O bonds (M=Al, Mg) indicating Si-O-M bonding. On further heating at 1200°C, the band at 780 cm^{-1} corresponding to the ring structure of the SiO_4 tetrahedron appears.²⁴

3.1c Phase evolution (XRD): Figure 5 shows XRD patterns for the pure cordierite (PCZr0) sample at different sintering temperatures. The results reveal that the sintering temperature as an important parameter in the synthesis. The XRD results for pure cordierite sample indicated the presence of a metastable μ -cordierite at low sintering

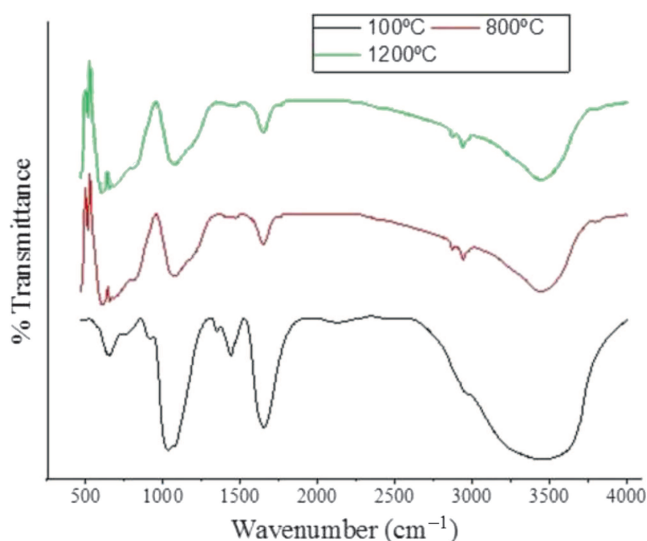


Figure 4. FTIR spectrum of cordierite–zirconia (PCZr20) samples at different sintering temperatures.

temperatures and a stable high-temperature α -cordierite as a major constituent phase in all the samples. The μ -cordierite is present as a glassy phase in the metastable state. It is observed in the temperature range between 800 and 1200°C. The complete transformation of α -cordierite phase was observed at 1350°C.¹⁹

The XRD results of cordierite–zirconia (PCZr20) are shown in figure 6. The results were found to be identical with pure cordierite, that is formation of α -cordierite phase. In addition to the α -cordierite phase, ZrSiO₄ formation is due to the reaction of ZrO₂ with SiO₂ at 1350°C. The presence of α -cordierite and zircon at sintering temperature of 1350°C for 3 h has a significant effect. The purpose of the addition of zirconia to form a secondary phase is the basis for this research to study the improvement in mechanical properties.

The XRD interpretation for cordierite ceramics prepared from mixtures of clay minerals studied at 1300°C. This illustrated the presence of the main phase cordierite and the secondary crystalline phases.²⁹ The cordierite samples sintered at 1300 and 1350°C for 1 h indicated³⁰ the presence of cordierite. Significant amounts of cristobalite, spinel and traces of corundum were also reported. The sintering at 1400°C for 1 h exhibited the complete disappearance of cristobalite, spinel and corundum. For the increased sintering time of 3 and 5 h, similar results were observed for the samples sintered at 1350°C.

3.2 Thermo-mechanical, physical property studies for cordierite and cordierite–zirconia ceramic samples

The results of thermal and mechanical properties of the cordierite and cordierite–zirconia composites sintered at various sintering temperatures up to 1350°C are discussed in the following sections.

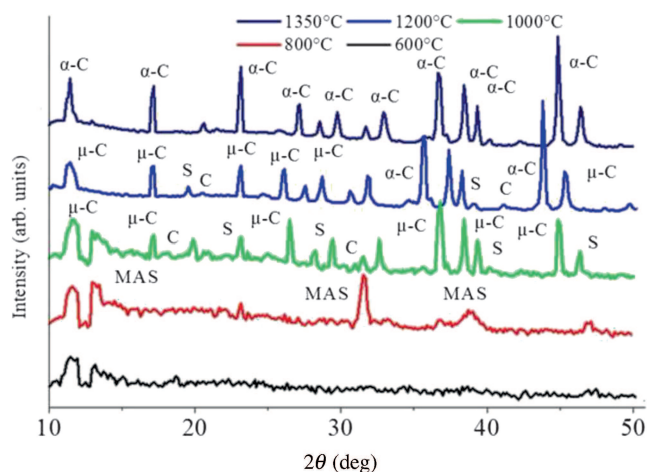


Figure 5. XRD patterns for pure cordierite (PCZr0).

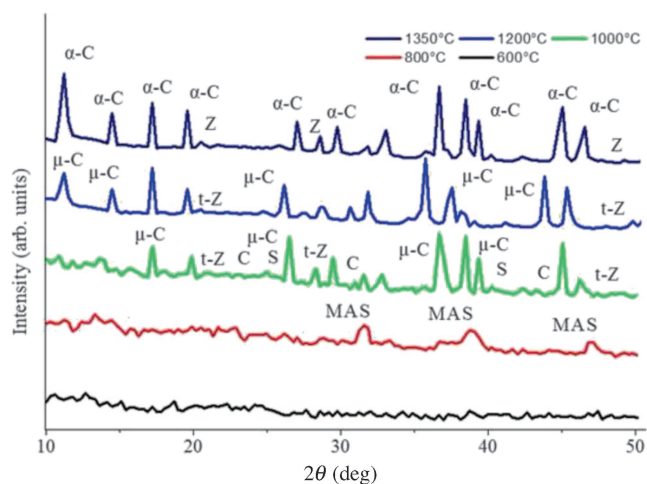


Figure 6. XRD patterns for cordierite–zirconia (PCZr20).

3.2a Bulk density and porosity: The bulk density of the cordierite compacts prepared by the precipitation and conventional route densified rapidly between 1000 and 1100°C (figure 7). Since, the crystallization of spinel occurs because of the intimately mixed Al³⁺ and Mg²⁺ ions, densification has occurred by the formation of some viscous liquid within a very short temperature range. The curve indicates that the densification of cordierite powder stops at the onset of the crystallization of μ -cordierite. The crystallization of cordierite takes place when the compacts are fired for longer duration of time. It should be noted that in order to obtain denser products, sintering of the compacts must precede crystallization as the reverse would greatly decrease the mobility of the ions and impede sinterability. In this case, crystallization of cordierite takes place after the compacts have sintered completely.

The cordierite exhibited abrupt densification in this temperature range.^{31,32} However, by increasing the sintering temperature further, densification stopped. The amorphous

silica component crystallizes to α -quartz. At sintering temperatures above 1100°C resulted in decrease in densification up to 1350°C. This shows the complete transformation of α -cordierite. For the samples prepared by precipitation and conventional method at consolidation temperature reported a similar result. The cordierite pellets sintered above 1300°C, reported increase in vapour pressure of the water. It expands the cavities and pores within the compacts. This makes it difficult to locate the temperature range. The densification was achieved without a detectable crystallization. The moderate densities were developed in samples.^{33,34} The results of porosity analysis (figures 7 and 8) for pure cordierite by the precipitation technique has confirmed, that the porosity decrease was evident up to 1100°C and on further heating porosity was found to increase. The results confirm that bulk density of samples decreased slightly (figure 7). The result of

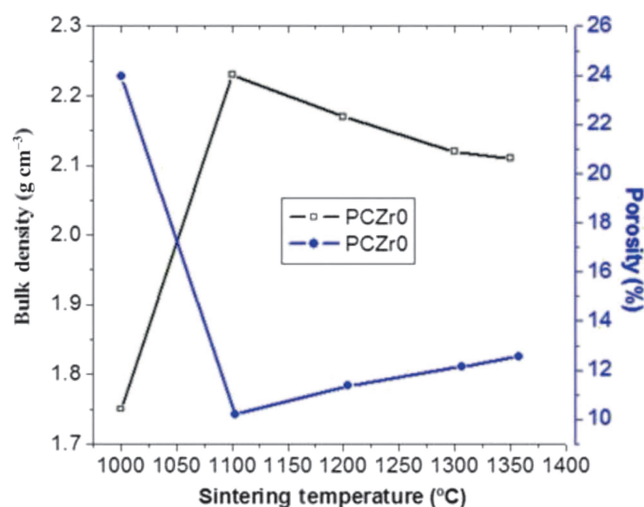
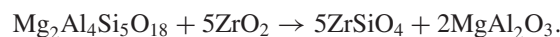


Figure 7. Bulk density and porosity of pure cordierite at different sintering temperatures.

porosity analysis is also in agreement with the densification results of the sample PCZr0.

Figure 9 shows that for a given zirconia content (PCZr05–PCZr20) the density increased with sintering temperature. Further, at a given sintering temperature, the density increased with zirconia content in the cordierite–zirconia composite. The results exhibit that the densification temperature reduces by the addition of zirconia. The bulk density of the composites slightly increased with the increase in zirconia content in all series of composite samples. The ceramic containing 20 wt% of zirconia (PCZr20) shows the maximum bulk density.

The cordierite samples in the presence of ZrO_2 reported the enhanced densification.^{35,36} The sample PCZr20 in this research showed that the bulk density increased with the increase in temperature. Further with the increased amount of zirconia content. During the sintering of the cordierite–zirconia composites, two processes occur, namely densification and the formation of spinel and zircon phases. Following is the reaction at the sintering temperature for cordierite–zirconia composites containing 15 and 20 wt% of zirconia, forming zircon and spinel between cordierite and zirconia:



It is observed from the X-ray diffraction patterns (figure 6) of all present samples, that the intensity of the zircon phase is slightly higher by the increased amount of ZrO_2 with an increase in the sintering temperature. It is obvious that the discrepancies in the densities of all series of cordierite–zirconia ceramic, are due to the formation of zircon with the presence of $t\text{-ZrO}_2$ in the matrix. The above results have been verified from the studies of porosity analysis for zirconia–doped cordierite (PCZr20) samples by the precipitation technique shown in figure 10. The porosity decreased with increase in the sintering temperature, and shows that the

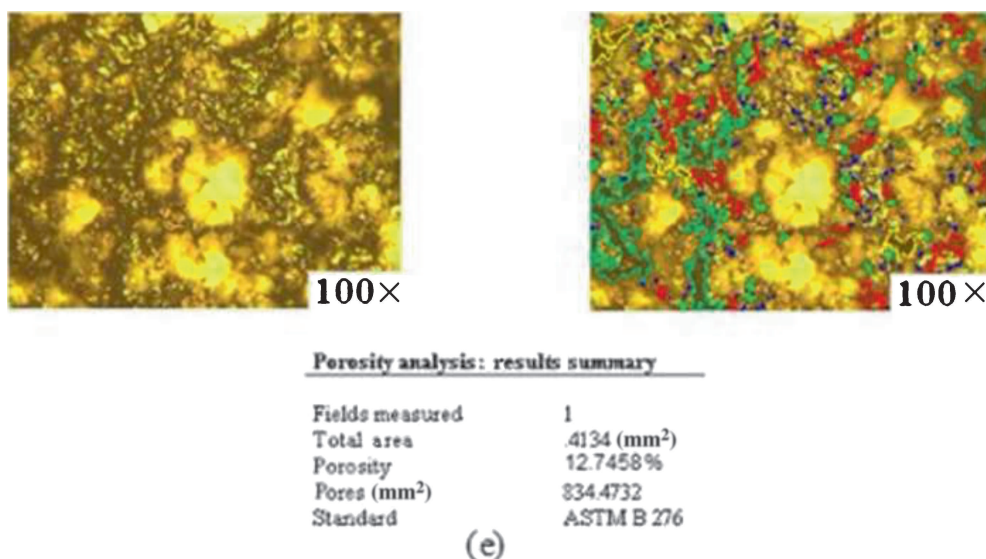


Figure 8. Porosity analysis of pure cordierite at 1350°C.

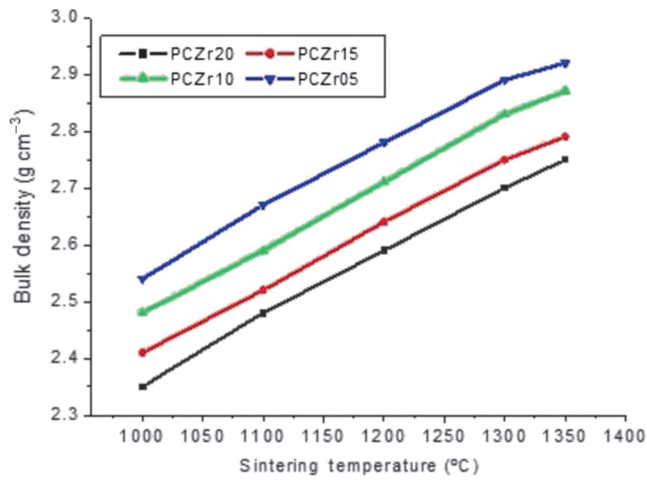


Figure 9. Bulk density of cordierite–zirconia at different sintering temperatures.

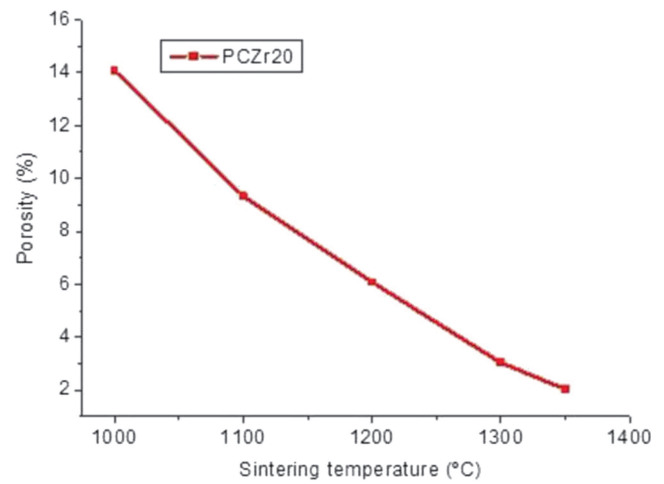


Figure 10. Porosity of cordierite–zirconia (PCZr20) at different sintering temperatures.

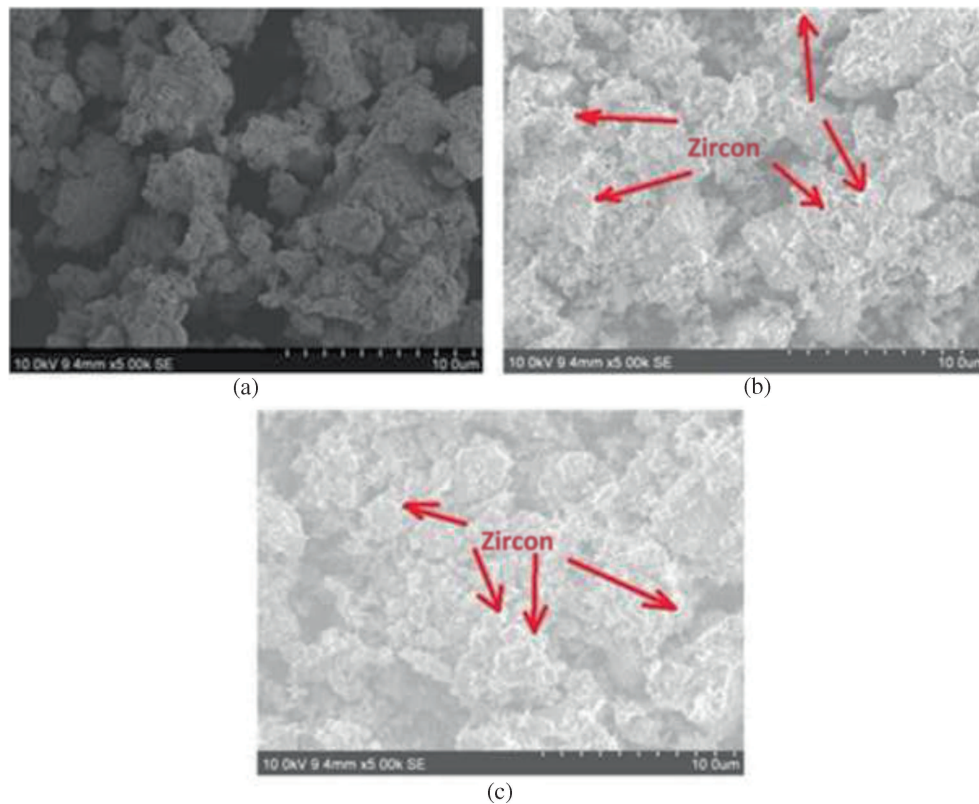


Figure 11. SEM photographs of ceramic samples sintered at 1350°C: (a) PCZr0, (b) PCZr20 and (c) PCZr20.

good densification results are obtained. The sample PCZr20 reported the lowest porosity, which showed good densification. This shows that porosity is in the opposite trend to the bulk density. The porosities of the PCZr20 sample sintered at 1350°C are very less.

3.2b Microstructural studies: Figure 11a shows the photomicrograph of cordierite specimen, which displays the

surface morphology of a sintered cordierite compact with an appreciable amount of porosity. This is in agreement with the measured density. In addition, the micrograph reveals the different sizes of the grains, that densification begins by liquid phase sintering or a viscous flow mechanism prior to crystallization. It is interesting to note that the initial cordierite grain does not change its size and the corners remain sharp, indicating that little dissolution and precipitation take place

during densification. The densification of cordierite ceramics in this study is concluded to be achieved in the first stage of liquid-phase sintering, i.e., melt redistribution and particle rearrangement. It is also interesting to note that the round-shaped cristobalite particles observed in the sample PCZr0. They began to disappear with increasing cordierite formation. This inhibition occurs as a result of the formation of a reaction layer around each alumina particle in the cordierite.

Figure 11b and c reveals the photomicrograph of cordierite–zirconia composites (PCZr05 and PCZr20) containing 5 and 20 wt% of zirconia sintered at 1350°C. The microstructure of the composite samples shows a uniform spatial distribution of the dispersed zirconia particles in the cordierite matrix, which demonstrates the advantages of the precipitation processing route, characterized by various-sized grain morphology with the presence of micro-pores and grain boundaries. The existing pores at the grain boundaries in early and intermediate stages are pulled together to form a large pore in the final stage of sintering. The XRD pattern shows the presence of both zircon and t-zirconia phases, but in the SEM, no clear distinction between the zircon and zirconia particles is observed.

3.2c Hardness determination: Figure 12 shows the Vickers hardness values of pure cordierite samples (PCZr0) for an applied load of 98 N as a function of the sintering temperature. The hardness of pure cordierite (PCZr0) showed an increase in hardness up to 1100°C due to the formation of μ -cordierite at this temperature. The hardness was found to decrease with sintering temperature above 1100°C. This could be due to the formation of α -cordierite and spinel phases. The Vickers hardness of cordierite sample sintered at 1350°C was found to be 6.91 GPa.³⁷

The zirconia-doped cordierite samples sintered at 1350°C showed that the hardness increased with the increase in the sintering temperature and also with increase in the zirconia content (CZr05–CZr20) as shown in figure 12. The toughening of oxide by dispersion in ceramics by a secondary phase is a well-established process, and has been successfully employed to improve the mechanical properties. Hence, zirconia added with cordierite, forms zircon as a secondary phase. This shows that the hardness value of cordierite–zirconia (20 wt%) is found to be 7.68 GPa, which showed an increase from 7.06 to 7.68 GPa. This is an expected result in the ceramics as the crystalline phases are usually harder. However, the research on cordierite and cordierite–zirconia synthesized by the precipitation technique tried with the addition of a different binder (carboxymethyl cellulose) also exhibited better results.³⁸

3.2d Fracture toughness estimation: Figure 13 shows the fracture toughness of pure cordierite (PCZr0) sample heat treated at different temperature. The fracture toughness of pure cordierite material is high ($K_{IC} = 2.94 \text{ MPa m}^{1/2}$) at 1100 and above 1100°C. There is a decrease in fracture toughness value of $2.73 \text{ MPa m}^{1/2}$. This may be due

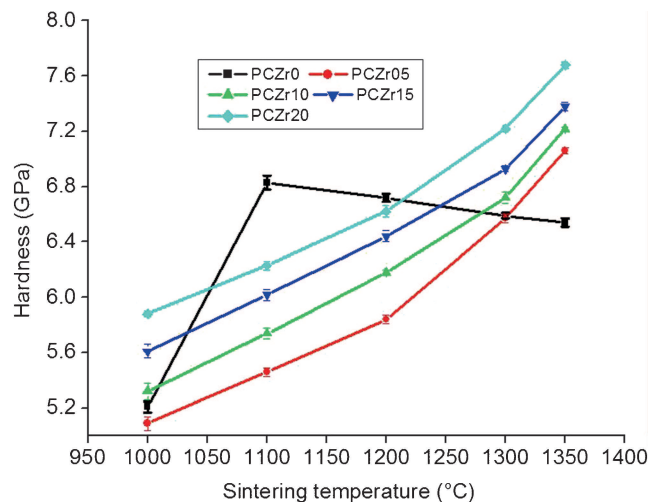


Figure 12. Vickers hardness of pure cordierite and cordierite–zirconia sintered at different temperatures.

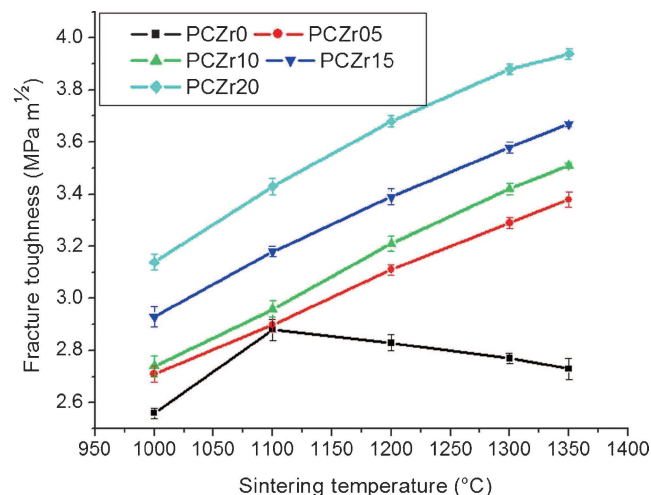


Figure 13. Fracture toughness of pure cordierite and cordierite–zirconia sintered at different temperatures.

to the formation of α -cordierite above 1000°C. Higher grain growth results in lowering of the fracture toughness above the sintering temperature at 1200°C.

The fracture toughness of the cordierite is enhanced with the addition of ZrO_2 (5–20 wt%). Generally, toughening of ceramics with the addition of ZrO_2 can be achieved through martensitic transformation from tetragonal to monoclinic phase with t- ZrO_2 . There were no ZrO_2 and cordierite to form ZrSiO_4 phase, as confirmed by the XRD analysis (figure 6). The fracture toughness of the cordierite–zirconia composites is shown in figure 13.

The fracture toughness of the cordierite–zirconia ceramic is higher at 1350°C. This may be due to the decrease in the t- ZrO_2 phases. The toughening was partly attributed to the residual compressive stresses imposed on the cordierite due to thermal expansion mismatch between cordierite and ZrSiO_4 particles, especially at higher amount of stabilized

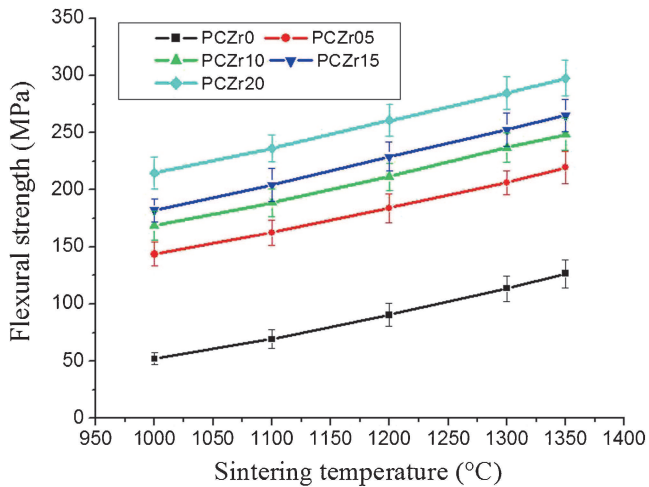


Figure 14. Flexural strength of pure cordierite and cordierite–zirconia sintered at different temperatures.

zirconia. This shows that the fracture toughness value of ceramic for the addition of 20 wt% of ZrO₂ was 3.94 MPa m^{1/2}. This research shows better than the fracture toughness by the indentation method, for the sintered bodies containing the various amounts of zirconia. The fracture toughness increased from 2.1 MPa m^{1/2} for pure cordierite to 3.2 MPa m^{1/2} at a content of 35 wt% of ZrO₂, which suggested that both the fracture strength and toughness depend on the amount and the phase type of zirconia.¹²

3.2e Testing for flexural strength: The data on the flexural strength of pure cordierite and cordierite–zirconia are shown in figure 14. The flexural strength of pure cordierite (PCZr0) ceramic samples were obtained for samples heat treated at various sintering temperature. The results reveal that the flexural strength of pure cordierite increases from 52.13 to 126.46 MPa with the increase in sintering temperature, which may be due to the α -cordierite formation at this temperature.¹²

The flexural strength of cordierite–zirconia ceramic (PCZr05–PCZr20) increased from 219.54 to 297.62 MPa with the addition of 5–20 wt% of zirconia; this is shown in figure 14. It can be seen that the flexural strength increased gradually with the increase in zirconia content. Several toughening mechanisms may occur simultaneously in zirconia toughened composites. The stress-induced transformation from the tetragonal phase to the monoclinic phase is known as the most effective toughening mechanism for zirconia reinforced matrix ceramic composites. However, even if the martensitic transformation toughening mechanism will not prevail, other toughening mechanisms like microcracking and crack deflection are expected to be active. The cordierite–zirconia presented an increase in strength up to 1350°C. The observed results were found to be better than the previous research¹² who studied the mechanical behaviour of cordierite–zirconia composites by co-precipitation process. The reported results show that the addition of ZrO₂ to pure cordierite, increased the fracture strength from 110

to 260 MPa. The flexural strength were closely related to the microstructure and dependent on the amount and the phase type of zirconia (tetragonal or monoclinic).

3.2f Thermal expansion coefficient evaluation: The results for the cordierite (PCZr0) samples show that the thermal expansion coefficient is $2.48 \times 10^{-6} \text{ }^{\circ}\text{C}^{-1}$ at 70°C increases slightly to $4.08 \times 10^{-6} \text{ }^{\circ}\text{C}^{-1}$ at 800°C. The reason for this increase is due to the presence of cristobalite possibly formed by the crystallisation of amorphous silica. Coefficient of thermal expansion (CTE) of CZr0 measured showed that there is a little difference between the measured and reported.³⁹

The thermal expansion coefficient increased from 0.52×10^{-6} to $4.42 \times 10^{-6} \text{ }^{\circ}\text{C}^{-1}$ for the cordierite–zirconia sample (PCZr20) in the same temperature range. The addition of zirconia into the cordierite matrix increased the CTE monotonously. The slight increase of CTE for PCZr20 is due to the dispersion of ZrO₂ in the cordierite matrix. As it is believed that the thermal expansion may be affected by the porosity content. The cordierite crystals with high porosity can cause expansion and contraction easily. This statement could explain why the thermal expansion of denser cordierite bodies are slightly higher than those with higher residual porosity. The CTE obtained for the composite was based on the sum of the coefficient of ZrSiO₄ in the matrix and that of the cordierite matrix.¹⁵ The CTE of ZrSiO₄ is $4.1 \times 10^{-6} \text{ }^{\circ}\text{C}^{-1}$. Particles of larger CTE in a matrix of lower CTE cause thermal strain (tension), which results in the genesis of micro-cracks in the matrix around the particles. The results indicate that micro-cracks between the cordierite matrix and ZrSiO₄ particles were generated during the first cooling, resulting in a decrease of thermal expansion.

4. Conclusion

From the results of the above study, conclusions drawn are as follows:

1. Pure cordierite and cordierite–zirconia (5–20 wt%) under controlled composition was successfully synthesized.
2. Densified cordierite–ZrO₂ was prepared by dispersing 20 wt% of zirconia at sintering temperature 1300°C and the addition of zirconia decreased the optimum sintering temperature at 1400°C.
3. The fracture toughness of 3.94 MPa m^{1/2} with a hardness of 7.68 GPa combined with a flexural strength of 297.62 MPa was observed in the cordierite–zirconia sample (PCZr20) that exhibited the highest value.
4. Addition of zirconia showed a better thermal expansion coefficient, a value which is considered to have a negligible effect on cordierite sample.

Acknowledgements

We would like to thank the Department of Mechanical Engineering, Anna University, Chennai 600025 and SMBS, VIT

University Chennai 600127, India, for providing the facilities to carry out this research work.

References

- Shamsudin Z, Hodzic A, Soutis C, Hand R J, Hayes S A and Bond I P 2011 *J. Mater. Sci.* **46** 5822
- Okada A 2008 *J. Eur. Ceram. Soc.* **28** 1097
- Williams J L 2001 *Catal. Today* **69** 3
- Trumbolic L J, Acimovic Z, Panic S and Andric L J 2003 *FME Trans.* **31** 43
- Stoyanova D D, Vladov D Ch, Kasabova N and Mekhandzhiev D R 2005 *Kinet. Catal.* **46** 609
- Kazakos A M, Komarneni S and Roy R 1990 *J. Mater. Res.* **5** 1095
- Pavlikov V M, Garmash E P, Yurchenko V A, Pleskach I V, Oleinik G S and Grigor'ev O M 2011 *Powder Metall. Met. Ceram.* **49** 564
- Gibbs G H 1996 *Mineral* **51** 1068
- Montorsi M A, Delorenzo R and Verne E 1994 *Ceram. Int.* **20** 353
- Li P, Du Y and Hu L 2002 *Refractory* **36** 139
- Zhou L, Wang C and Liu W 2009 *Rare Met. Mater. Eng.* **38** 366
- Hirano M and Inada H 1993 *J. Mater. Sci.* **28** 74
- Senthil Kumar M and Elayaperumal A 2013 *Int. J. Mater. Res. Technol.* **7** 99
- Shu C, Mingia X, Cailou Z and Jiaqi T 2002 *Mater. Res. Bull.* **37** 1333
- Awano M and Takagi H 1994 *J. Mater. Sci.* **29** 412
- Sun E H, Choa Y-H, Sekino T and Niihara K 2002 *Ceram. Int.* **6** 105
- Ponton C B and Rawlings R D 1989 *Mater. Sci. Technol.* **5** 865
- Djordjevi N and Pavlovi L 2006 *J. Serb. Chem. Soc.* **71** 293
- Tang B, Fang Y W, Zhang S R, Ning H Y and Jing C Y 2011 *Indian J. Eng. Mater. Sci.* **18** 221
- Pal D, Chakraborty A K and Sen S 1996 *J. Mater. Sci.* **31** 3995
- Senguttuvan G, Settu T, Kuppusamy P and Kamaraj V 1999 *J. Mat. Synth. Proc.* **7** 175
- Weikusat C, Glamacher U, Miletich R, Neumann R and Trautmann C 2008 *Nucl. Instrum. Methods: Phys. Res. B* **266** 2990
- Naskar M K and Chatterjee M 2004 *J. Eur. Ceram. Soc.* **24** 3499
- Janackovic D, Jokanovic V, Kostic-Gvozdenovic L, Zec S and Vskokovic D 1997 *J. Mater. Sci.* **32** 163
- Radev L, Samunova B, Mihailova I, Pavlova L and Kashchieva E 2009 *Proc. Appl. Ceram.* **3** 125
- Hinklin T and Laine R 2008 *Chem. Mater.* **20** 553
- Petrovic R, Janackovic D, Zec S, Drmanic S and Kostic-Gvozdenovic L J 2003 *J. Sol-Gel Sci. Technol.* **28** 111
- Saha S K and Pramanik P 1995 *J. Mater. Sci.* **30** 2855
- Valaskova M and Martynkova G S 2009 *Chem. Pap.* **63** 445
- Goren R, Ozgur C and Gocmez H 2006 *Ceram. Int.* **32** 53
- Vesteghem H, Di Giampado A R and Dauger A 1987 *J. Mater. Sci. Lett.* **6** 1187
- Higgins R I, Bowen H K and Giess E A 1987 In *Ceramic powder science* (eds) G L Messing, K S Mazdiyasm, J W Mc Cauley and R A Haber (Columbus, OH, USA: American Ceramic Society) Vol 21, p 691
- Mussler B H and Shafer M W 1985 *J. Am. Ceram. Soc. Bull.* **64** 1559
- Suzuki H, Ota K and Saito H 1987 *J. Ceram. Soc. Jpn.* **95** 170
- Travitzky N A and Claussen N 1988 *Adv. Ceram.* **23** 121
- Niezery K and Weisskopf K L Petzow 1988 *Sci. Sinter.* **20** 149
- Penkov I, Pascova R and Drangajova I 1997 *J. Mater. Sci. Lett.* **16** 1544
- Senthil Kumar M, Elayaperumal A and Senguttuvan G 2011 *J. Ovonic Res.* **7** 99
- Yamuna A, Johnson R, Mahajan Y R and Lalithambika M 2004 *J. Eur. Ceram. Soc.* **24** 65